Sustainable whey proteins-nanostructured zinc oxide-based films for the treatment of chronic wounds: New insights from biopharmaceutical studies

Sustainable Whey proteins-Nanostructured zinc oxide-based films for the treatment of chronic wounds: new insights from biopharmaceutical studies

Paolo Pino[1#], Barbara Vigani[2#], Caterina Valentino[2], Daiana Ianev[2], Marco Ruggeri[2], Cinzia Boselli[2], Antonia Icaro Cornaglia[3], Pietro Grisoli[2], Barbara Onida[1], Francesca Bosco[1], Giuseppina Sandri[2], Silvia Rossi[2]**

[1]Department of Applied Science and Technology, Politecnico di Torino, 10129 Turin, Italy;

[2]Department of Drug Sciences, University of Pavia, 27100 Pavia, Italy.

[3]Department of Public Health Experimental and Forensic Medicine, University of Pavia, 27100 Pavia, Italy

[#] These authors equally contributed to the present work

KEYWORDS: bionanocomposite, whey proteins based films, antibacterial properties, cell proliferation, wound healing

ABSTRACT: Chronic wounds represent silent epidemic affecting a large portion of the world population, especially the elders; in this context, the development of advanced bioactive dressings is imperative to accelerate wound healing process, while contrasting or preventing infections. The aim of the present work was to provide a deep characterization of the functional and biopharmaceutical properties of a sustainable thin and flexible films, composed of whey proteins alone (WPI) and added with nanostructured zinc oxide (WPZ) and intended for the management

of chronic wounds. The potential of whey proteins-based films as wound dressings has been confirmed by their wettability, hydration properties, elastic behavior upon hydration, biodegradation propensity and, when added with nanostructured zinc oxide, antibacterial efficacy against both Gram-positive and Gram-negative pathogens, i.e. *Staphylococcus aureus* and *Escherichia coli*. *In-vitro* experiments, performed on normal human dermal fibroblasts, confirmed film cytocompatibility, also revealing the possible role of Zn^{2+} ions in promoting fibroblast proliferation. Finally, *in-vivo* studies on rat model confirmed film suitability to act as wound dressing, since able to ensure a regular healing process while providing effective protection from infections. In particular, both films WPI and WPZ are responsible for the formation in the wound bed of a continuous collagen layer similar to that of healthy skin.

1. INTRODUCTION

Chronic wounds represent a major and often overlooked problem for healthcare [1]: in the last 5 years, chronic wounds have become a serious life-threatening disease, showing a comparable mortality rate to cancer [2]. Several factors, especially metabolic disorders, aging, vascular deficits, trauma and severe infectious disease (i.e. COVID-19), may worsen primary wounds, prolonging their healing process [3, 4]; additionally, delayed wound management has been of particular concern during the COVID-19 pandemic, increasing the risk of infections [5]. In most cases, chronic wounds are exacerbated by the high exposure to infections, which are responsible for worsening the patient's health and extending the duration of hospital stays. In an alarmingly increasing number of cases, pathogenic bacteria are also found to be poorly sensitive to both systemic and topical antimicrobial therapy because of widespread antibiotic resistance [6].

This scenario calls for urgent action, especially concerning the development of advanced wound dressings capable of contrasting or preventing infections, while promoting healing [7,8].

To address the antibiotic resistance, the research on new antimicrobial agents has demonstrated the potential of nanostructured materials, such as metal-oxide one [9,10]. Nanostructured zinc oxide (nZnO) is a promising nanomaterial with renowned antimicrobial, antioxidant, and anti-inflammatory properties [11]. The release of Zn^{2+} ions represent the principal mechanism of antimicrobial action of nZnO, as well as the production of reactive oxygen species and the physical interactions with bacterial cells [12,13]. Moreover, zinc is an essential trace element for the human body and takes an active part in wound healing, supporting re-epithelialization and skin modelling [14]. All these properties make nZnO a particularly promising filler for the preparation of biopolymer-matrix composite (defined as bionanocomposite), although concerns still exist about the potential cytotoxicity of its nano-sized form [15, 16].

Whey proteins, particularly in the form of Whey Protein Isolate (WPI), are obtained from whey, that is the most important by-product of the dairy industry: the disposal of a large amount of whey as wastewater involves serious environmental hazards and represents a significant loss of potential ingredients, such as lactose, fat and proteins. In an attempt to exploit the whey value and to mitigate its harmful effects on the environment, it seemed useful to direct whey management towards a sustainable way of utilization, such as the production of novel valuable products [17]. Whey proteins represent a promising biomaterial known for its biodegradability and bioactivity [18]: It contains high levels of amino acids, such as arginine, glycine, leucine, isoleucine and valine, which are essential in the promotion of wound healing, and proline, that is considered pivotal for collagen biosynthesis, structure and strength [19]. For thirty years now, whey proteins are known for their excellent film-forming ability driven by the formation of hydrophobic interactions and intermolecular disulfide bridges upon protein denaturation [20]. In particular, whey proteins have recently gained attention in the food packaging industry: such biopolymers are involved in the formation of edible films, endowed with outstanding mechanical (i.e. flexibility) and barrier

properties (i.e. high water vapor permeability and excellent oxygen permeability), which serve as a functional food-environment barrier ensuring food safety and quality [21,22].

All these properties suggest that whey proteins could be used for the fabrication of sustainable and innovative wound dressings; actually, there are no published studies on the use of whey proteins-based films for wound healing applications. Nowadays, only an oral supplementation with whey proteins has been proposed as an interesting strategy to integrate the local treatment of wounds [23,24].

A previous work of ours demonstrated how whey proteins and nZnO can be combined by a simple procedure to obtain flexible and antibacterial films based on WPI-nZnO bionanocomposite for biomedical and food packaging applications [25]. The present work further expands on this research by investigating some peculiar features of whey proteins-based films and WPI-nZnO bionanocomposite-based films (i.e. film morphology, hydration propensity, biodegradation behavior and antibacterial efficacy against *S. aureus* and *E. coli)*, which could be relevant for their use in wound healing application. In fact, to the best of our knowledge, it is the first time that whey proteins-based films with and without nZnO were proposed as innovative wound dressings and characterized for their biopharmaceutical properties both *in-vitro* and *in-vivo*. Moreover, in the present work the *in-vitro* effects of the films on human dermal fibroblast viability and proliferation are investigated, and an *in-vivo* test is ultimately carried out on a murine model to prove their wound healing potential.

2. MATERIALS AND METHODS

2.1. Materials. Zinc acetate di-hydrate (≥ 98%), potassium hydroxide (≥ 85%), and absolute ethanol were obtained from Sigma-Aldrich (St. Louis, MO, USA) and used as received. Whey Protein Isolate (WPI) was kindly supplied by Milei GmbH (Leutkirch im Allgäu, Germany).

2.2. Synthesis of nZnO. nZnO was obtained from wet chemical precipitation as reported in [25]. Zinc acetate dihydrate (29.50 g) and potassium hydroxide (14.80 g) were dissolved in 120 mL and 64 mL of ethanol respectively, and subsequently mixed and kept at 60°C for 72 h under stirring and reflux. The white precipitate was recovered by means of a 30 min centrifugation cycle at 1073 g (ALC PK110 centrifuge; DJB Labcare Ltd, Newport Pagnell, England) and subsequently washed three times with ethanol and dried overnight at 60°C.

2.3. Preparation of whey proteins-based films (WPI films) and WPI-nZnO bionanocomposite-based films (WPZ). WPI and WPZ films have been prepared according to the procedure previously described in [25] (Figure 1). Briefly, a 10% (w/w) WPI suspension was prepared in distilled water and its pH was brought to 7.0 with dropwise addition of 1 M NaOH. The suspension was heat-treated at 70°C for 20 min in a thermostatic bath under constant stirring and subsequently cooled down in a water bath at room temperature. A glycerol amount equal to 60% (w/w) of the dry protein weight contained in the suspension was added as plasticizing agent. The so-obtained film-forming solution was then casted onto non-stick molds maintaining a volume-to-surface ratio equal to 0.135 m, and finally dried for 2.5 h at 60°C. This allowed to obtain WPI films. For the preparation of WPZ films, a mass of nZnO equal to 4% (w/w) of the dry protein weight was dispersed in distilled water and sonicated in an ultrasound bath for 1 h. The nanoparticles suspension was then mixed with the heat-treated film-forming solution right after the addition of glycerol, and the resulting mix was casted and dried.

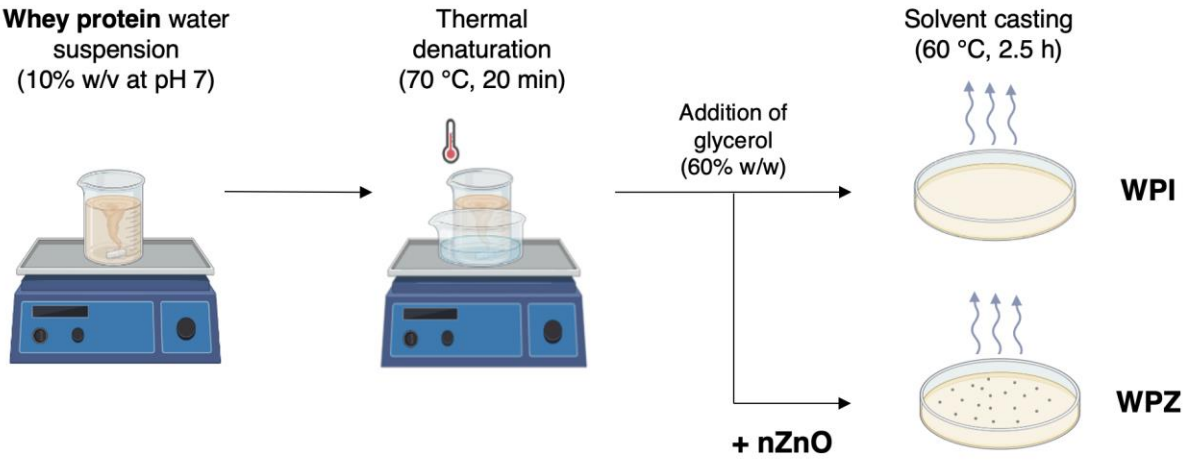

Figure 1. Schematic representation of solvent-casting method for the preparation of WPI and WPZ films.

2.4. Microstructural Analyses. Morphological evaluation of WPI and WPZ films was performed by means of a scanning electron microscope (Phenom Pure G6 SEM, ThermoFisher Scientific, Waltham, MA, USA), equipped with LUXOR Gold-Coater. Different magnifications were considered for each film. Film topography and nZnO distribution into WPZ matrix were assessed by means of Atomic Force Microscopy (Tosca 200, Anton Paar, Graz, Austria) in tapping mode (cantilever AP-ARROW-NCR, Silicon SPM-Sensor, Al-coating; thickness: 4.6 µm, length: 160 µm, width: 45 µm); tapping mode images were acquired with a resonance frequency equal to 285 kHz and force constant of 42 N/m. The resulting data were transformed into a 3D image. The mean surface roughness (S_a) of WPI and WPZ films was also calculated.

2.5. Water Contact Angle Measurements. Water Contact Angle (WCA) was measured using a DMe-211 Plus Contact Angle Meter (Kyowa Interface Science Co Ltd., Saitama, Japan) according to the $\theta/2$ method. For the test, a drop (10 μL) of Phosphate Buffer Solution (PBS, pH 7.4; Biosolve Chimie, Dieuze, France) was deposited onto the surface of WPI and WPZ samples

and the contact angle was measured over time at 1 s intervals using FAMAS Dropmaster Software. The experiment was repeated five times.

2.6. Hydration test. A hydration test was carried out to monitor water uptake of the film over time. An experimental set-up has been designed to simulate the contact conditions between the films and an exuding wound area. The wells of a polypropylene plate (Corning® 12 Well TC-Treated Microplates, New York, NY, USA) have been filled to the brim with PBS. Subsequently, a sheet of Parafilm® has been applied over the plate and pierced in correspondence of the PBS-filled wells, allowing the liquid to emerge and to form a wet layer on the Parafilm®. WPI and WPZ films have been cut in circular specimens with the same diameter of the wells, dried in an oven at 60°C until stabilization of the weight, and applied on top of an equally shaped dialysis membrane. The experimental set-up used for the hydration test allowed to safely manipulate the films across the entire duration of the experiment without compromising their integrity. Membrane-supported film specimens have thus been placed on the wet Parafilm®, and the entire set-up was placed inside an incubator at 32°C to simulate the temperature of the skin. To measure the swelling ratio (SR), specimens were collected, blotted away of excess water with a filter paper, and weighted. The SR was then determined according to the following equation:

$$SR = \frac{m_w - m_d}{m_d} \times 100$$

where m_w is the wet mass and m_d is the dry initial mass. The swelling ratio has been calculated after 1, 3, 6 and 24 h. The experiment has been done in triplicate.

2.7. Viscoelastic Properties after Hydration. After 24 h hydration, dynamic oscillatory measurements were performed by means of a rotational rheometer (MCR102, Anton Paar, Turin, Italy), using a parallel plate combination (PP25, diameter = 25 mm) as measuring system. Stress sweep test was performed at 1 Hz frequency to identify the linear viscoelastic region (LVR). In the oscillation test, a shear stress equal to 1 Pa (within the LVR previously determined) was applied

150 at increasing frequencies (1 to 10 Hz) and G' (storage modulus) and G" (loss modulus) profiles
151 were recorded; measurements were performed at 32°C. Three replicates were considered for each
152 sample.

153 **2.8. Degradation test.** The degradation profile of WPI and WPZ films was investigated by
154 soaking the samples in two different degradation media: PBS [26] and H_2O_2 500 μM in PBS [27].
155 In detail, WPI and WPZ circular specimens have been dried at 60°C until stabilization of the
156 weight (30 ± 5 mg) and subsequently immersed in 5 mL of PBS or H_2O_2 500 μM in PBS. Immersed
157 films have been kept at 32°C for the duration of the entire experiment.

158 After 1, 3 and 7 days, sample degradation was evaluated in terms of (i) film residual mass and
159 (ii) protein concentration dissolved in the degradation media.

160 In particular, films have been collected and dried in an oven at 60°C until stabilization of the
161 weight. The percentage of residual mass (R) has been determined as:

162 $$R = \frac{m_0}{m_f} \times 100$$

163 where m_f is the final residual dry mass and m_0 is the dry initial mass. The experiment has been
164 repeated three times.

165 Thereafter, the amount of protein fraction dissolved in each medium as a consequence of film
166 degradation was determined by means of UV-Vis spectroscopy analysis (spectrophotometer UV-
167 vis Lamba 25, Perkin Elmer, Milan, Italy) at $\boldsymbol{\lambda}$ = 280 nm; this method is particularly useful and
168 offers high specificity for proteins that contain tryptophan or tyrosine residues such as whey
169 proteins [28].

170 A calibration curve was used to determine the protein concentration in the medium after film
171 degradation: solutions containing increasing concentrations (from 0.001 to 1 mg/ml) of
172 denaturated WPI were prepared. Three replicates were considered for each sample.

2.9. Antimicrobial test. The antibacterial activity of WPI and WPZ films was investigated against *Staphylococcus aureus* ATCC 6538 (Gram-positive) and *Escherichia coli* ATCC 10356 (Gram-negative). Before testing, the microorganisms were grown overnight in Tryptone Soya Broth (Oxoid; Basingstoke, Hampshire, England) at 37°C. Washed cells were resuspended in Dulbecco's PBS and optical density (OD) was adjusted to 0.3, corresponding approximately to 110^8 Colony Forming Units (CFU/ml) at 650 nm wavelength.

Ten µl of bacterial suspension was placed on a standard glass slide (76 × 26 mm); the microbial suspension was, then, covered with WPZ film (20 × 20 mm), forming a thin film that facilitates direct contact of the microorganisms with the active WPZ surface. The assembled glasses were introduced in a Falcon test-tube (50 ml) containing 1 ml of PBS to maintain a damp environment; the WPZ surfaces were maintained in contact with the liquid films containing bacteria at room temperature for 6 and 24 hours; for each time of contact, WPI film was treated in the same way, as control sample. After the times of contact, 9 ml of PBS were introduced in each Falcon test-tube under a gentle shaking to detach the glass slides from WPZ and WPI surfaces. Bacterial suspensions were then grown in Tryptone Soya Agar to count viable cells. The decimal-log reduction rate, microbicidal effect (ME), was calculated using the following equation:

$$ME = \log NC - \log NE$$

where NC is the number of CFU/ml developed on the control glasses (WPI film), whereas NE is the number of CFU/ml counted after exposure to WPZ surfaces. The results expressed as ME represent the average of three equivalent determinations [29,30].

2.10. *In-vitro* cytocompatibility test. Normal Human Dermal Fibroblasts (NHDF) from juvenile foreskin (PromoCell GmbH, VWR, Milan, Italy) from 6^{th} to 12^{th} passage were used. Cells were cultured in polystyrene flasks in Dulbecco's Modified Eagle's Medium (DMEM), supplemented with 10% v/v heat-inactivated Foetal Bovine Serum (FBS) (VWR International

197 S.r.l, Milan, Italy), and with 1% v/v antibiotic-antimycotic solution (Merk Life Science S.r.l.,
198 Milan, Italy), at 37°C in 5% CO_2 atmosphere.

199 Extraction dilution method was performed to investigate the cytotoxic effect of WPI and WPZ
200 films [31]. More in detail, WPI and WPZ specimens (0.32 cm^2), previously sterilized through UV
201 irradiation, were soaked in 600 µL of complete culture medium (CM) for 24 h at 37°C for obtaining
202 film extracts; then, the extracts were collected and serially diluted (1:2, 1:10, 1:50, 1:100 v/v) by
203 adding fresh CM.

204 Fibroblasts was seeded at a density of 1.0×10^5 cells/well into a 96-well plate and incubated
205 (37°C and 5% CO_2) for 24 h in order to reach semi-confluence. After the medium had been
206 replaced with the extracts, as such or diluted, the cells were incubated for a further 24 h; CM was
207 used as a reference. After incubation, an MTT assay was performed. Briefly, extracts and reference
208 were removed from the 96-well plate and cell monolayers were washed with Phosphate Buffer
209 Solution (PBS); subsequently, 50 µl of MTT 7.5 µM in 100 µl of DMEM without phenol red were
210 added to each well and incubated for 3 h (37°C and 5% CO_2). Finally, 100 µl of DMSO was added
211 to each well in order to promote the complete dissolution of formazan crystals, obtained from MTT
212 dye reduction by mitochondrial dehydrogenases of living cells. The solution absorbance was
213 measured by means of an iMark® Microplate reader (Bio-Rad Laboratories S.r.l.) at a wavelength
214 of 570 nm and 690 nm (reference wavelength) after 60 s of mild shaking. Six replicates were
215 considered for each sample.

216 **2.11. *In-vitro* proliferation test.** The extracts, obtained as previously described at 24 h, were
217 also investigated for their capability to enhance NHDF proliferation at 1, 3 and 7 days. Cells were
218 seeded into a 96-well plate at a density of 2.0×10^4 cells/50 µL of CM/well and immediately added
219 with 150 µL extracts diluted 1:2 v/v with fresh CM. CM was used as a reference. Finally, an MTT
220 test was performed as described in the previous paragraph. Six replicates were considered for each

sample. Results were expressed as cell viability % by normalizing the absorbance measured after contact with each sample with that measured for CM, used as reference. Six replicates were performed for each sample/control.

2.12. *In-vivo* studies

2.12.1 Evaluation of wound healing-enhancing properties on rat model. All animal experiments were carried out as previously described [32] in full compliance with standard international ethical guidelines (European Parliament 2013) (European Communities Council Directive 86/609/EEC) approved by the Italian Health Ministry (Italian Health Ministry 2021). The study protocol was approved by the Local Institutional Ethics Committee of the University of Pavia for the use of animals.

In brief, male rats (Wistar 200–250 g) (n=4) were anesthetized with equitensine (3 mL/kg) and shaved to remove all hair from the site of injury. Three full-thickness burns were produced on the animal's back by contact with a brass rod (105°C for 40 s), having a circular diameter of 4 mm. After 24 h, three 6-mm full-thickness excisional wounds were outlined using a punch biopsy tool on each animal back. Wounds were photographed with a digital camera and then treated with i) WPI film (0.32 cm^2) moistened with 25 µL of saline (NaCl 0.9% w/v), ii) WPZ film (0.32 cm^2) moistened with 25 µL of saline and iii) 25 µL of saline as control. Subsequently, each wound was covered with a sterile gauze and the rat's back was wrapped with a surgery stretch (Safety, Monza, Italy), to keep films or the physiological solution into the wound bed. At prefixed times after treatment (3, 7, 14, and 18 days), the three lesions were photographed with a digital camera in order to monitor wound healing process. The wound healing potential of WPI and WPZ films was evaluated by wound area retraction (%) using the following equation:

$$\text{Wound area retraction (\%)} = (A_t/A_0) \times 100$$

where A_0 is the initial wound area and A_t is the wound area at different time points; the wound area was determined using the imaging analysis program ImageJ 2.0.

2.12.2 Histological analysis. After 18-day treatment, the animals were sacrificed. After euthanasia, the area around the scar or residual wound was harvested and wound tissue specimens (wound bed) were immediately immersed in the fixative solution (4% neutral buffered formaldehyde), embedded in paraffin and sectioned at a thickness of 5 μm. Some sections were stained with hematoxylin and eosin (H&E), others with picrosirius red (PSR).

Picrosirius polarization method is one of the best understood techniques of collagen histochemistry and it is particularly useful to reveal the organization and the heterogeneity of collagen fiber in different connective tissues. Polarizing light assessment of PSR stain identified the old thick collagen I fibers as orange-to-red and the newly deposed, rich in collagen III fibers, as green [33,34]. Picrosirius red stain was applied as follows: deparaffinized sections were hydrated, faintly stained with Weigert's hematoxylin for nuclei and stained with PSR (1 hour). Then all sections were dehydrated, cleared in xylene and mounted with DPX (dibutyl phthalate in xylene).

Stained slices were observed with a light microscope Carl Zeiss Axiophot (Oberkochen, Germany) provided, for circular polarizing microscopy, with suitable filters in the condenser stage and in the microscope tube. Images were recorded through a microscope digital 5 megapixels CCD camera Nikon DS - Fi2.

2.12. Statistical analysis. Whenever possible, experimental data were subjected to statistical analysis, carried out by means of the statistical package Statgraphics 5.0 (Statistical Graphics Corporation, Rockville, Maryland, USA). In particular, one-way ANOVA was carried out followed by a Multiple Range Test.

3. RESULTS AND DISCUSSION

Whey Protein Isolate-based films, endowed with optimal barrier properties and the capability to load various functional agents (i.e. antimicrobials and prebiotics/probiotics), have increasingly attracted the attention of the scientific community, sometimes outperforming polysaccharide- and other protein-based films [22]. In recent years, the use of biopolymers, obtained from renewable sources or industrial by-products, in the manufacturing of flexible and edible films for food packaging has proved to be an environmentally friendly and sustainable strategy to replace petroleum-based packaging materials [35]. Besides the well-known whey proteins nutritional value, the numerous health benefits of WPI encourage researchers to develop new WPI-based therapeutic platforms intended for different biomedical purposes [18, 36]. In particular, WPI appears to be a valuable candidate for the production of dressings for wound healing applications [37]. It contains a high level of amino acids, both essential and non-essential ones, which are involved in protein synthesis, and it is a rich source of glutamine required to support cellular growth and proliferation [38]. Moreover, the addition of nZnO into WPI-based films, as proposed in our previous work [25], could appear useful for treating skin wounds; in fact, it is reported in the literature that ZnO nanoparticles have been successfully used in wound dressings thanks to their strong antimicrobial properties following cutaneous application and their epithelialization-stimulating effect [11,39].

In the present work, a biopharmaceutical characterization of the developed WPI and WPI-nZnO bionanocomposite-based films was performed both *in vitro* and *in vivo* to investigate film properties that are relevant for clinical applications in wound healing.

3.1. Microstructural morphology and surface topography

Figure 2A reports SEM micrographs of WPI and WPZ films. WPI film was characterized by a smooth, compact and homogeneous surface, as opposed to WPZ bionanocomposite film that showed a rough surface with evenly distributed nZnO (average particle size equal to 32 nm and

specific surface area of approximately 47.3 m^2/g). SEM micrographs highlight the presence of some aggregates of nZnO, which appear as shiny spots within WPZ film structure [40]. The formation of irregular nZnO aggregates is probably due to the high nanoparticle surface energy and occurs during solvent evaporation [25, 41, 42]. The topography of film surface was also investigated by AFM and results, as 2D and 3D images, are also shown in Figure 2B. Some aggregation of nZnO is responsible for an increase in roughness with the creation of deep valleys and high peaks; these results confirm SEM microstructural observations. S_a expresses, as an absolute value, the difference in height of each point compared to the arithmetical mean of the surface and, thus, is generally used to quantitatively define the surface roughness. S_a was 3.40 nm for WPI film and 79.4 nm for WPZ film, proving the presence of nZnO within biopolymer-based structure. Figure 2C shows the macroscopic appearance of WPI and WPZ films, endowed with an optimal flexibility and, thus, suitable for topical application on skin wounds.

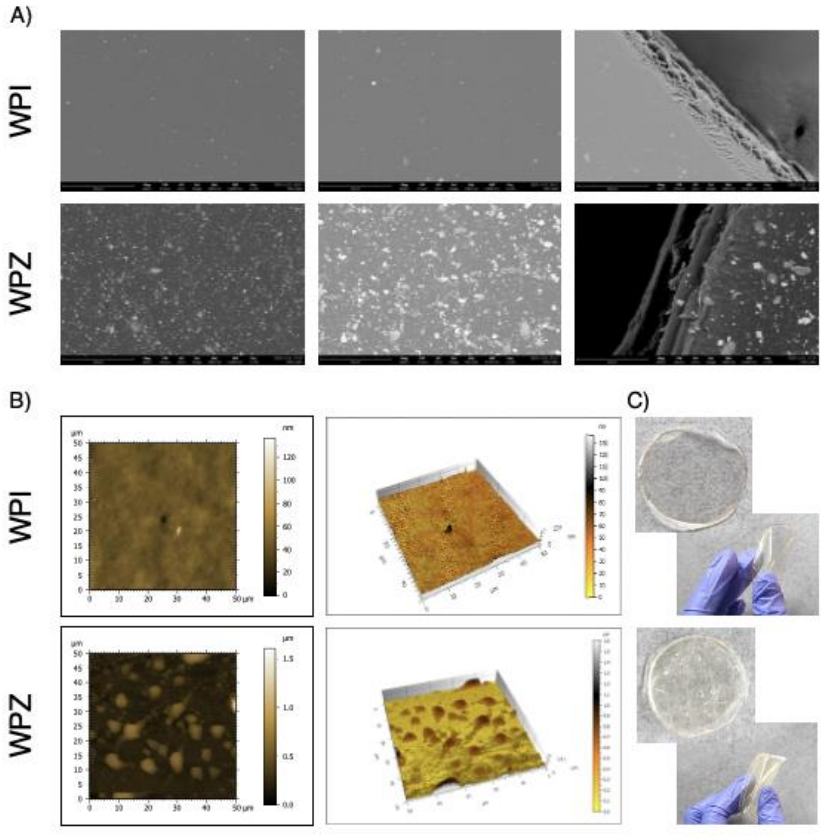

Figure 2. SEM micrographs (A) and 2D and 3D AFM images (B) of WPI and WPZ films. C) Macroscopic appearance of WPI and WPZ films.

3.1. Water Contact Angle. The surface wettability of whey proteins-based films, in presence and in absence of nZnO, was evaluated by means of water contact angle (WCA) analysis. The results of the WCA measurements are shown in Figure 3.

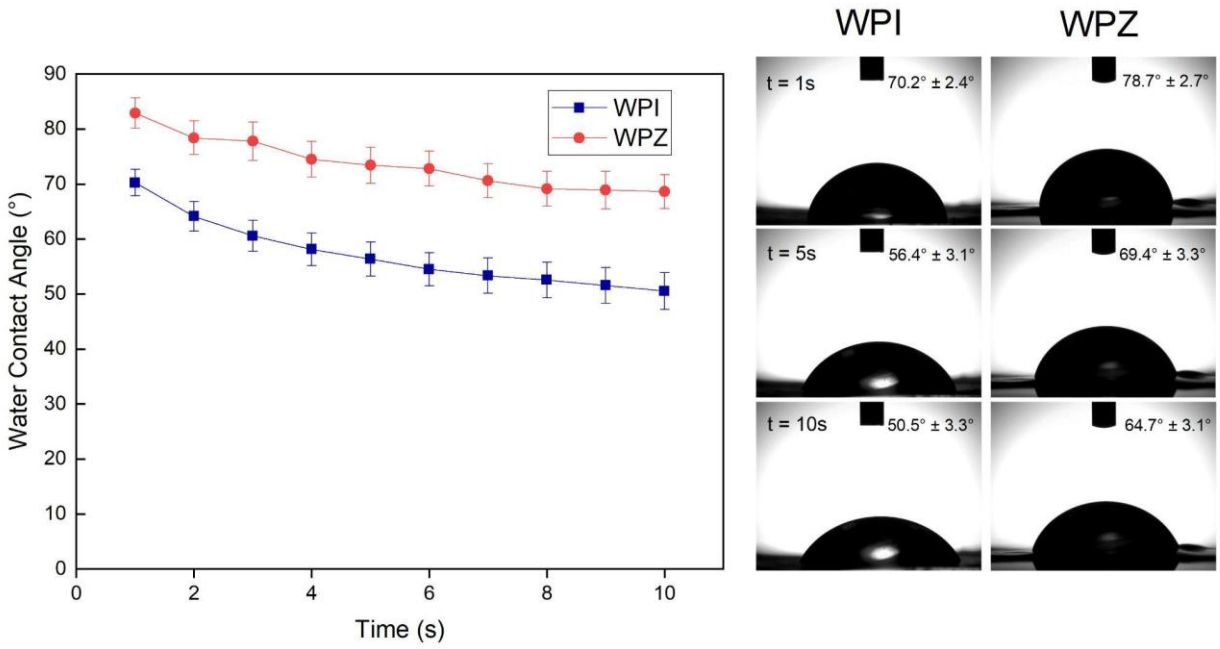

Figure 3. WCA values of WPI and WPZ films up to 10 s (mean values ± S.D.; n = 3). Images of the drop at different times (1, 5, and 10 s) are reported for WPI and WPZ films.

As shown by the WCA values lower than 90°, both samples are hydrophilic. The addition of nZnO causes a significant increase in WCA values (p-value < 0.05) in the time interval under investigation. Such behavior is frequently observed for other biopolymer/nZnO nanocomposites described in the literature [39, 43-45]. The reduced wettability of WPZ film can be related to both the hydrophobic nature of nZnO incorporated into the biopolymer-based film and the increase in WPZ surface roughness, appreciated in SEM and AFM images (Figure 2); in fact, it is well-known that roughness makes hydrophobic surfaces more hydrophobic [46].

Moreover, Figure 3 shows that the value of WCA decreases over time in both samples. Thanks to the overall good water affinity of the bionanocomposite, the droplet tends to spread across the surface of the films, thus determining a decrease of WCA. After 10 s, the surface of both samples starts deforming due to the absorption of the liquid droplet, which prevents longer-duration measurements of the contact angle. WPI films were characterized by an initial WCA value equal to 70.2° ± 2.4° that decreases to 50.5° ± 3.3° after 10 s. In WPZ film, WCA has an initial value of 78.7° ± 2.7°, which goes down to 64.7° ± 3.1° after 10 s. The results obtained are in line with the literature since, generally, an ideal wound dressing is characterized by WCA value in the range of 50-70°. Hydrophilicity is obviously a fundamental property for primary dressings, i.e., those dressings that are placed in direct contact with the wound, in order to ensure exudate absorption and good adhesion to the site. Hydrophilic dressings ensure support and protection to the wound, reducing possible complications and accelerating the healing process [47,48].

3.2 Hydration test. The swelling ratio (SR) values were calculated for WPI and WPZ films upon 24 h (Figure 4), allowing a quantitative evaluation of the ability of the film to absorb a medium-simulating wound exudate (PBS) over time.

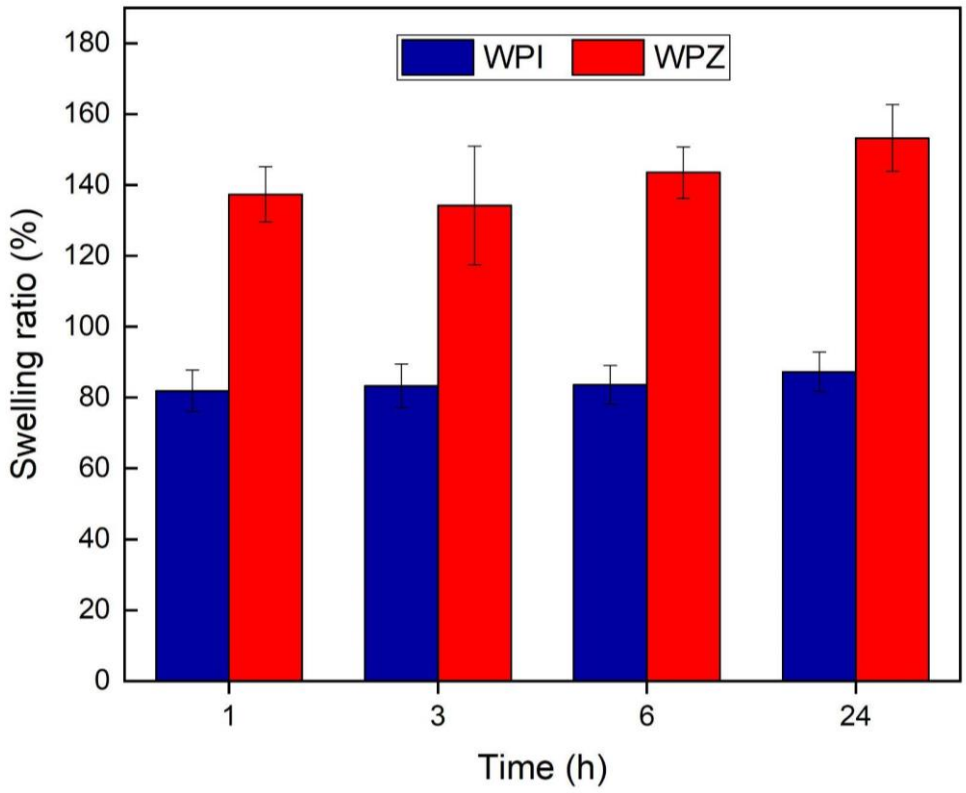

335

336 **Figure 4.** Variation in time of the swelling ratio % of WPI and WPZ films (mean values ± S.D.; n
337 = 6).

338 It can be noticed that WPZ samples showed higher (more than 1.5 times) SR values than WPI
339 films. This is in agreement with previous studies [25] as well as with other scientific reports [48-
340 50]. The increased SR value is attributed to the electrostatically charged surface of nZnO, which
341 attracts ions in the PBS inducing a build-up of osmotic pressure inside the WPI matrix, in tum
342 causing a higher PBS uptake.

343 Fluid uptake capability is an important parameter to be investigated for elucidating the film
344 behavior after application at the injury site [26]. Indeed, a wound dressing should preserve a moist
345 wound environment without enabling the accumulation of exudate, which could impair the healing
346 process and be responsible for the maceration of the healthy surrounding tissue [51,52]. Generally,
347 an ideal wound dressing must be characterized by SR values ranging between 100-900% [51,52].

Water uptake is rapid and occurs within the first 30 minutes, and then remains relatively stable or slightly increasing throughout the whole experiment. For WPI films, SR is 81.88% ± 5.85% after the first hour and becomes 87.25% ± 5.52% after 24 h. In WPZ, SR has an initial value of 137.36% ± 7.83%, which goes up to 153.26% ± 9.38% after 24 h. This is an important feature for wound dressings, as it demonstrates film stability for a prolonged time. It is worth noting that the observed SR values are within the range reported in the literature as optimal [53,54].

3.3 Viscoelastic Properties after Hydration. The amount of PBS absorbed by both films reached an equilibrium without compromising the film structural integrity. After 24 h of hydration, WPI and WPZ films were subjected to viscoelastic measurements. As shown in Figure 5, both samples were characterized by higher G' (storage elastic modulus) values than G'' (loss viscous modulus) ones in the whole range of frequencies considered. Such behavior is highly desirable for a wound dressing: once hydrated, both films, endowed with marked elastic properties compared to viscous ones, are able to recover the deformation caused by external shear stresses and, thus, to effectively protect the injured area [51,55]. The presence of nZnO is responsible for higher G' and G'' values, in particular for frequencies higher than 7 Hz. Moreover, it can be observed that in presence of nZnO both G' and G'' are characterized by a higher dependence on frequency; this could be due to the fact that the inclusion of nZnO may disturb the WPI chain network, restricting polymer chain mobility and, thus, resulting in an enhancement of elasticity [56].

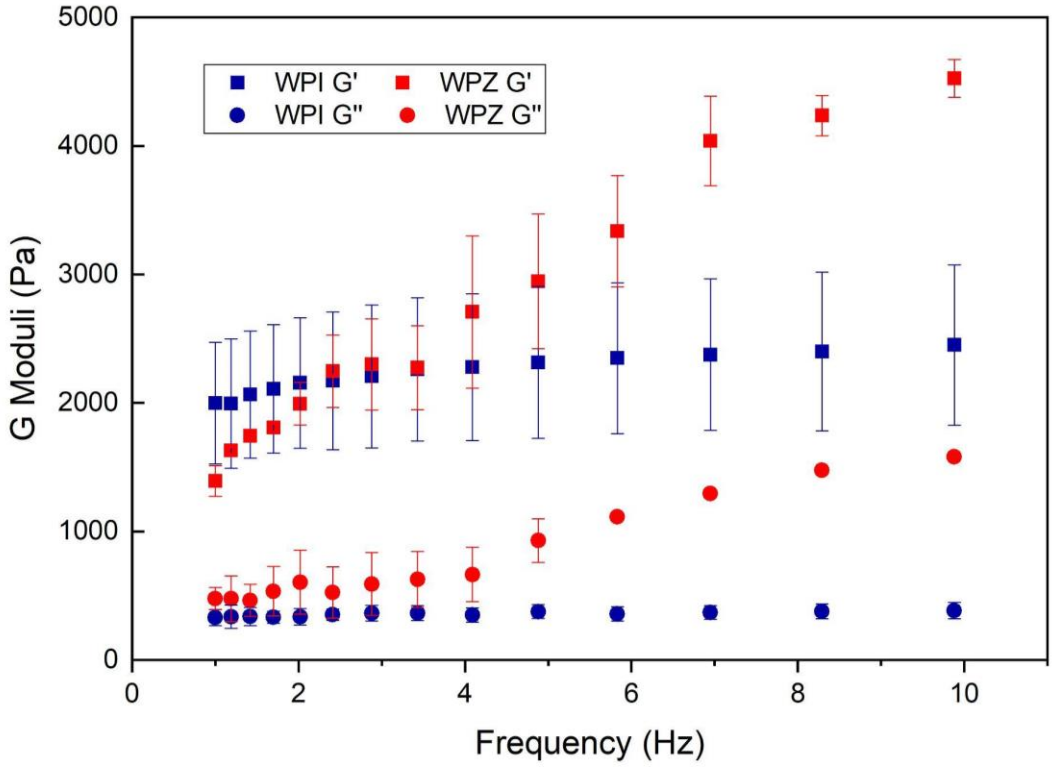

Figure 5. Storage (G') and loss (G") moduli vs. frequency profiles of WPI and WPZ films upon 24 h-hydration in PBS (mean values ± S.D.; n = 3).

3.4 Degradation test. The degradation rates of WPI and WPZ films over 7 days are shown in Figure 6. After 1, 3 and 7 days, sample degradation was evaluated in terms of (i) film residual mass (Figure 6A) and (ii) protein concentration dissolved in the degradation media (Figure 6B). Two different degradation media were considered: PBS (pH = 7.4), mimicking wound exudate, and PBS added with H_2O_2 to simulate the oxidative stress in the early inflammatory phase of the healing process [57,58].

The majority of the degradation occurs within the first day, while the further permanence of the samples in the medium (until 7 days) produced no significant additional mass loss (Figure 6A). It can therefore be hypothesized that the large mass loss occurring at the beginning is linked to the out-diffusion of weakly bonded molecules, such as glycerol, which are commonly present in WPI, as well as proteins that have not taken part in the formation of the film. After 7 days, what remains

is the robust intermolecular network composed of WPI proteins held together by more hydrophobic interactions and disulfide bridges [59]. The addition of H_2O_2 to PBS did not accelerate the degradation process, suggesting that both WPI and WPZ films are resistant to these oxidative conditions. These results are reflected by the protein concentration assessed in the degradation media, where higher protein content is observed in correspondence of those samples where lower residual mass was reported (Figure 6B).

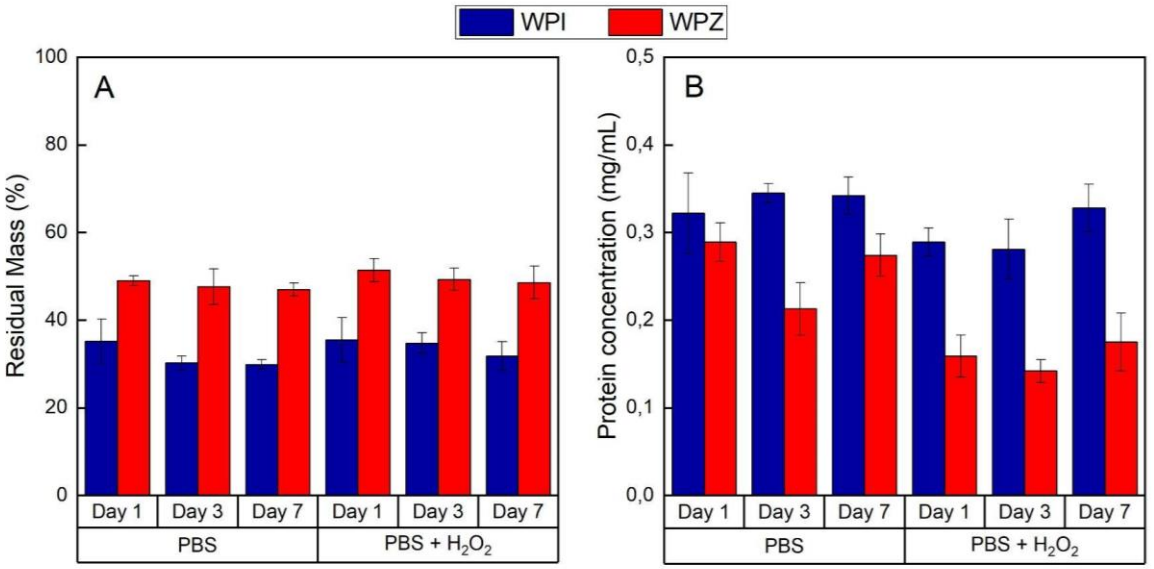

Figure 6. WPI and WPZ film degradation after 1, 3 and 7 days in two different media - PBS and PBS added with H_2O_2 - expressed in terms of (A) residual film mass and (B) concentration of proteins released in the medium (mean values ± S.E.; n = 3).

In order to increase film degradation time, the combination of proteins with polysaccharides might be a promising, thanks to the interactions between the two molecules [60].

As far as the effect of nZnO on the film stability is concerned, a few considerations can be made. The excess of residual mass measured for WPZ samples with respect to WPI ones (Figure 6A) appears systematically higher than the mass of nZnO alone in the samples, which would be equal to 4% of the dry mass in the conservative assumption that all the nZnO was retained inside the

matrix during degradation. These results strongly suggest that the presence of nZnO somehow limits the degradation of the film. This can be explained considering that nZnO stabilizes the matrix through its interactions with the whey proteins, preventing or slowing down their diffusion and dissolution in the medium [44, 61,62].

3.5 Antimicrobial test. The microbicidal effect (ME) of WPZ was evaluated on two different bacterial strains (*S. aureus* and *E. coli*); WPI film was used as a control reference. For both the microorganisms considered, WPZ film showed a microbicidal effect higher than WPI film; in particular, a marked antimicrobial effect of WPZ film was observed on *E. coli*.

Table 1. Microbicidal effect (ME) of WPZ after 6 and 24 h incubation with *S. aureus* and *E. coli*; WPI was used as control (CV % < 12%; n = 3).

	6 hours	**24 hours**
S. aureus	0.67	1.30
E. coli	2.85	4.94

These results reported in Table 1 confirm the well-known antibacterial properties of nZnO, but some interesting pieces of evidence emerge. In particular, a stronger effect against the Gram-negative was observed. The greater resistance of the Gram-positive to nZnO was attributable to their thicker peptidoglycan layer [12].

3.6 *In-vitro* cytocompatibility test. Film cytocompatibility was investigated by treating cells with the media in which WPI or WPZ films were soaked for 24 h at 37°C; such media were called film extracts. The results of the MTT assay carried on NHDF cells after 24 h incubation with film extracts are shown in Figure 7. All the film extracts were cytocompatible except for the non-diluted WPZ extract, as shown by the absorbance values reported in the graph. A very high concentration

of nZnO in the medium might in fact be detrimental for cells, as pointed out in several studies that raised concerns about the toxicity of metal oxide nanoparticles [63]. For ZnO nanoparticles, the release of Zn^{2+} ions has been considered the main toxicity mechanism on mammal cells, followed by the oxidative stress exerted by reactive oxygen species [15, 63]. However, cell viability is immediately restored with a 1:2 dilution and is preserved for all the subsequent dilutions. In fact, while toxic effects might arise at high concentrations, optimal amounts might allow to leverage the positive impact of zinc on the immune system and wound healing [11, 64, 65].

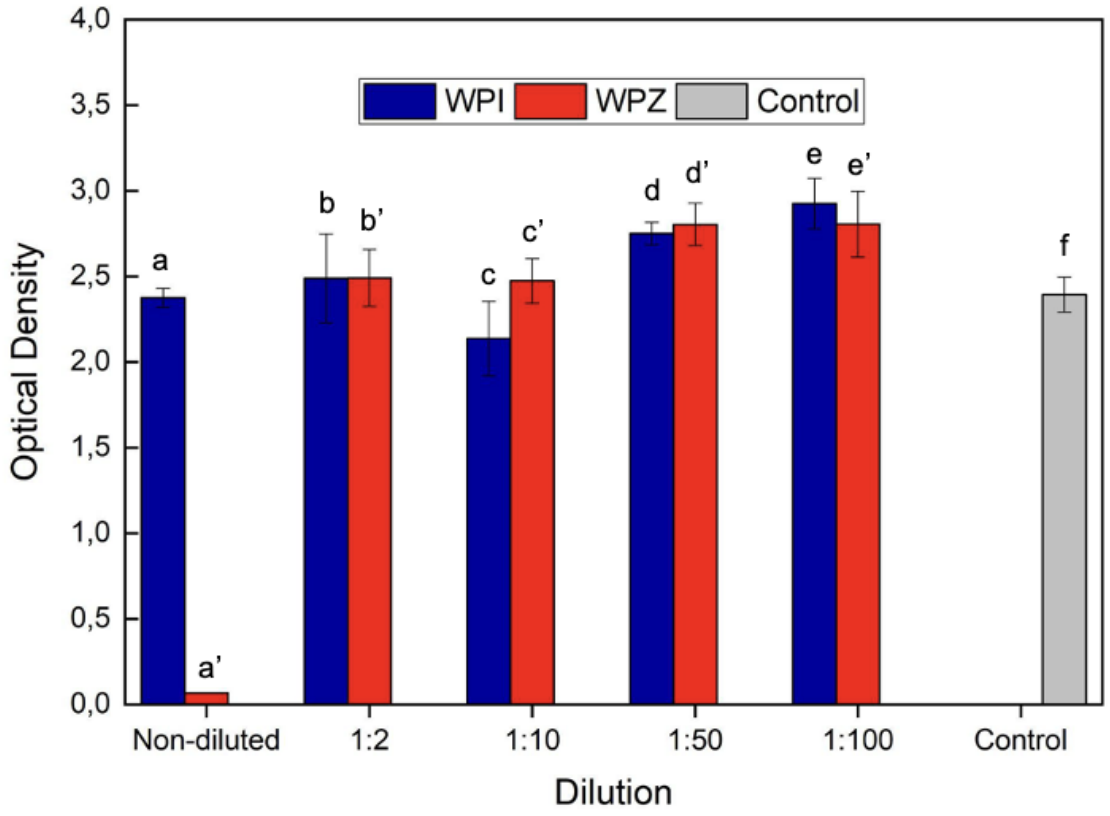

Figure 7. Optical density values after 24 h incubation of NHDF cells with WPI and WPZ extracts, undiluted and diluted 1:2, 1:10, 1:50, 1:100 v/v in CM. Complete culture medium (CM) was considered as control (mean values ± S.E.; n = 6). ANOVA one-way – Multiple Range Test (p-value ≤ 0.05): a vs a', e; c vs d, e; e vs f; a' vs b', c', d', e', f.

3.7 *In-vitro* proliferation test. Figure 8 shows the results of the MTT test performed after the *in-vitro* proliferation test carried on NHDF cells seeded using WPI and WPZ extracts, obtained after 1, 3 and 7 days and diluted 1:2 v/v in CM, as culture medium. WPZ induced a significantly higher proliferation compared to WPI and the control after 7 days of culture. This result, in accordance with the experimental evidence shown above (Figure 7), reveals the possible role of Zn^{2+} ions in fibroblast proliferation [14].

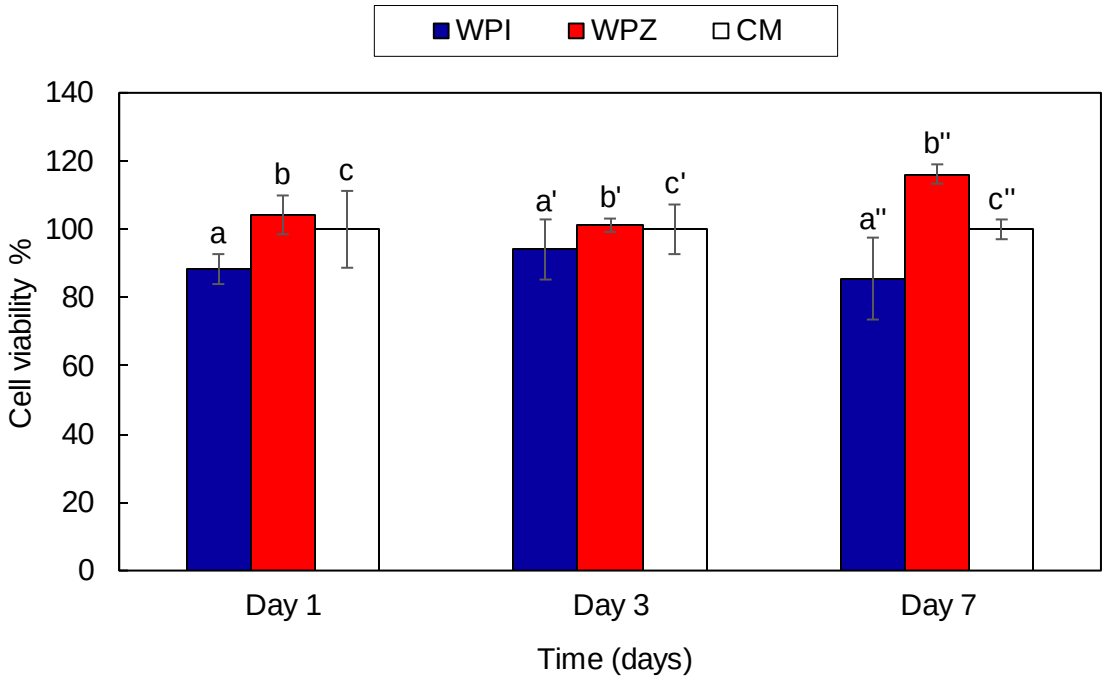

Figure 8. Viability % values after 1, 3 and 7 days of proliferation of NHDF cells in WPI and WPZ extracts, diluted 1:2 v/v in CM. Complete culture medium (CM) was considered as control (mean values ± S.E.; n = 6). ANOVA one-way – Multiple Range Test (p-value ≤ 0.05): a vs b; a'' vs b''; b'' vs c''; b vs b''; b' vs b''.

3.8 *In-vivo* wound healing test. As it can be seen in Figure 9C, WPI and WPZ treated wounds show signs of the proliferative phase of healing, with a number of blood vessels and a residual area of granulation tissue (a mixture of proliferating capillaries, fibroblast and inflammatory cells in a

loose edematous extracellular matrix). The entire surface of the lesion treated with the films was covered with new epithelium, fully restored in multiple layers of cells and with a fair degree of keratinization. Skin appendages such as hair follicles and glands were reforming. According to PSR staining, collagen was laid down and remodeled in an appropriate orientation to withstand the tensile stresses placed on the area of repair, suggesting a maturation and remodeling phase of the healing process [37,38,66]. A continuous collagen layer, rich in orange-to-red fibers, with a pattern similar to that of healthy skin, can be observed for WPI and WPZ treated wounds. Figure 9C highlights that the regeneration process is accelerated in wounds treated with whey proteins-based films with respect to saline. These results indicate that both WPI and WPZ films can be used as effective wound dressing nonetheless, as they ensure a regular healing process while providing effective protection from infections. After 18-day treatment, wound closure with completely regenerated epithelium was assessed in each sample (Figure 9B and D). No WPI or WPZ films nor portions of them could be observed, indicating a complete film biodegradation. This result suggests that the *in-vivo* degradation process of all the three matrices was suitable for the complete repair and regeneration of the injured skin tissue.

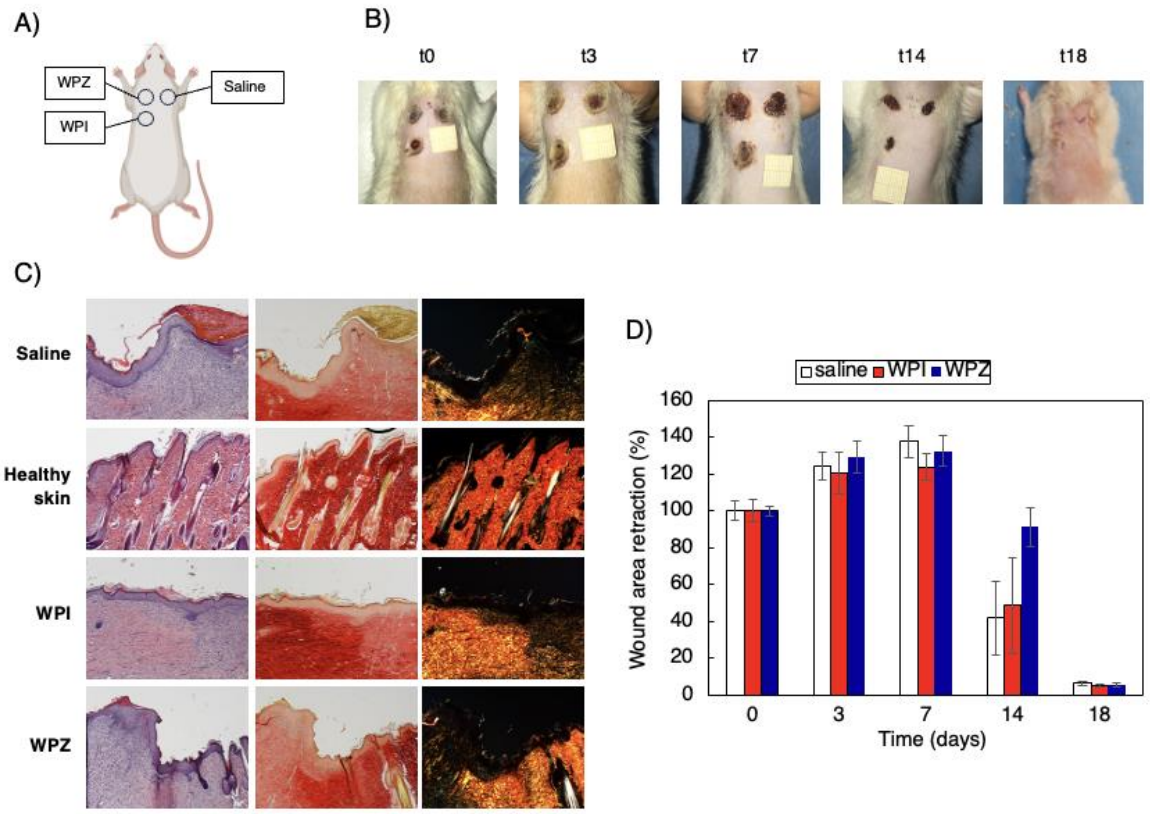

Figure 9. (A) *In vivo* wound healing model (murine burn/excisional model); (B) Photographical representation of wound healing in rats exposed to treatments on days (0, 3, 7, 14 and 18 days); (C) H&E (left panel) and PSR (central panel – with bright field images; right panel – with polarized light) sections of lesion treated with saline solution as negative control, healthy skin, lesion treated with WPI film and lesion treated with WPZ film. Original magnification: Original magnification: 5×. Each micrograph frame has a width of 1780 µm. Orange-to-red collagen fibers are visible in right panel. (D) Wound area retraction % vs. time obtained during the treatments (mean values ± S.E.; n = 4).

4. CONCLUSIONS

Wound healing and antimicrobial resistance are serious issues for global health. Elderly population is at high risk of developing chronic wounds due to the high prevalence of chronic

conditions, such as cardiovascular disease and diabetes, impaired mobility, incontinence, low weight, poor nutritional status, and cognitive impairment. Such chronic wounds are generally susceptible to hard-to-treat infections. Finding new wound dressings is imperative to alleviate these burdens and to improve the quality of life of millions of people. Since whey proteins are by-products of the dairy industry with well-known beneficial properties, they can be considered a valuable biomaterial candidate for the development of affordable and sustainable systems for tissue regeneration. Given these premises, the present work aimed: i) to prove the potential of WPI films as novel wound dressings; ii) to evaluate if the addition of nZnO in the whey proteins matrix provides antibacterial properties; iii) to investigate if the combination of WPI with nZnO in WPZ films synergically enhances wound healing. To achieve these aims, WPI and WPZ films have been subjected to a deep functional and biopharmaceutical characterization that showed how these films have wettability, hydration, degradation and rheological properties functional to their use as wound dressings. Such films were also characterized by cytocompatibility, fibroblast proliferation-enhancing properties and antibacterial activity. *In-vivo* studies confirmed their effectiveness to promote wound healing.

Further studies will be focused on the production of wound dressings based on novel biomaterials, consisting in complexes between whey proteins and polysaccharides, characterized by optimal biodegradability, ease workability and improved wound healing potential. Continuous manufacturing procedures, such as electrospinning, spray-drying and 3D-printing, will be considered to obtain fibrous membranes, microparticles and films, respectively, with a very low environmental impact.

ACKNOWLEDGEMENT

This research was partially supported by EU funding within the NextGenerationEU-MUR PNRR Extended Partnership initiative on Emerging Infectious Diseases (PE13 INF-ACT-F13C22001220007-PE00000007).

AUTHOR INFORMATION

Corresponding Author

Silvia Rossi

Department of Drug Sciences, University of Pavia, Via Taramelli 12, Pavia, 27100, Italy,

Tel +39 0382987357, Fax +39 0382422975, Email silvia.rossi@unipv.it

Barbara Onida

Department of Applied Science and Techonology, Politecnico di Torino, Corso Duca degli Abruzzi 24, Torino, 10129, Italy,

Tel +39 0110904631, Email barbara.onida@polito.it

Author Contributions

The manuscript was written through contributions of all authors. All authors have given approval to the final version of the manuscript.

ABBREVIATIONS

WPI, Whey Protein Isolate; nZnO, nanostructured ZnO; ROS, Reactive Oxygen Species; WCA, Water Contact Angle; PBS, Phosphate Buffer Solution; SR, Swelling Ratio; LVR, Linear Viscoelastic Region; R, Residual mass; OD, Optical Density; CFU, Colony Forming Units; ME, Microbial Effect; NHDF, Normal Human Dermal Fibroblasts; H&E, Hematoxylin and Eosin; PSR, Picrosirius Red.

REFERENCES

(1) M. Olsson, K. Järbrink, U. Divakar, R. Bajpai, Z. Upton, A. Schmidtchen, J Car, The humanistic and economic burden of chronic wounds: A systematic review. Wound Repair Regen. 27 (2019) 114–125. DOI: 10.1111/wrr.12683

(2) C. K. Sen, Human Wound and Its Burden: Updated 2020 Compendium of Estimates, Adv. Wound Care (New Rochelle) 10 (2021) 281-292. DOI: 10.1089/wound.2021.0026

(3) K. Las Heras, M. Igartua, E. Santos-Vizcaino, R. M. Hernandez, Chronic wounds: Current status, available strategies and emerging therapeutic solutions, J. Control Release 328 (2020) 532-550. DOI: 10.1016/j.jconrel.2020.09.039

(4) D. Li, W. Cao, Q. Zhou, X. Wu, X. Song, H. Qin, COVID-19 and primary wound healing: A new insights and advance, Int. Wound J. (2023). DOI: 10.1111/iwj.14324

(5) J. Balikji, P. Kiani, P. A. Hendriksen, M. M. Hoogbergen, J. Garssen, J. C. Verster, Impaired wound healing is associated with poorer mood and reduced perceived immune fitness during the COVID-19 pandemic: A retrospective survey, Health Sci. Rep. 5 (2022) e764. DOI: 10.1002/hsr2.764.

(6) M.A. Abushaheen, Muzaheed, A.J. Fatani, M. Alosaimi, W. Mansy, M. George, S. Acharya, S. Rathod, D.D. Divakar, C. Jhugroo, S. Vellappally, A.A. Khan, J. Shaik, P. Jhugroo, Antimicrobial resistance, mechanisms and its clinical significance, Dis. Mon. 66 (2020) 100971. DOI: 10.1016/j.disamonth.2020.100971

(7) E. Rezvani Ghomi, S. Khalili, S. Nouri Khorasani, R. Esmaeely Neisiany, S. Ramakrishna, Wound dressings: Current advances and future directions, J. Appl. Polym. Sci. 136 (2019) 47738. DOI: 10.1002/APP.47738

(8) R. Laurano, M. Boffito, G. Ciardelli, V. Chiono, Wound dressing products: A translational investigation from the bench to the market, Eng. Regen. 3 (2022) 182–200. DOI: 10.1016/j.engreg.2022.04.002

(9) S. Sharifi, M. J. Hajipour, L. Gould, M. Mahmoudi, Nanomedicine in Healing Chronic Wounds: Opportunities and Challenges, Mol. Pharm. 18 (2021) 550-575. DOI: 10.1021/acs.molpharmaceut.0c00346

(10) A. Pormohammad, N.K. Monych, S. Ghosh, D.L. Turner, R.J. Turner, Nanomaterials in Wound Healing and Infection Control. Antibiotics. 10 (2021) 473. DOI: 10.3390/ANTIBIOTICS10050473

(11) P.K. Mishra, H. Mishra, A. Ekielski, S. Talegaonkar, B. Vaidya, Zinc oxide nanoparticles: a promising nanomaterial for biomedical applications, Drug Discov. Today. 22 (2017) 1825–1834. DOI: 10.1016/J.DRUDIS.2017.08.006

(12) A. Sirelkhatim, S. Mahmud, A. Seeni, N. H. M. Kaus, L. C. Ann, S. K. M. Bakhori, H. Hasan, D. Mohamad, Review on Zinc Oxide Nanoparticles: Antibacterial Activity and Toxicity Mechanism, Nanomicro. Lett. 7 (2015) 219-242. DOI:10.1007/s40820-015-0040-x.

(13) P. Pino, F. Bosco, C. Mollea, B. Onida, Antimicrobial Nano-Zinc Oxide Biocomposites for Wound Healing Applications: A Review, Pharmaceutics 15 (2023) 970. DOI: 10.3390/pharmaceutics15030970.

(14) A.B.G. Lansdown, U. Mirastschijski, N. Stubbs, E. Scanlon, M.S. Ågren, Zinc in wound healing: Theoretical, experimental, and clinical aspects, Wound Repair Regen. 15 (2007) 2–16. DOI: 10.1111/J.1524-475X.2006.00179.X

(15) S. Sruthi, J. Ashtami, P.V. Mohanan, Biomedical application and hidden toxicity of Zinc oxide nanoparticles, Mater. Today Chem. 10 (2018) 175-186. DOI: 10.1016/j.mtchem.2018.09.008

(16) S. Karki, M. B. Gohain, D. Yadav, P. G. Ingole, Nanocomposite and bio-nanocomposite polymeric materials/membranes development in energy and medical sector: A review, Int. J. Biol. Macromol. 193 (2021) 2121-2139. DOI: 10.1016/j.ijbiomac.2021.11.044.

(17) E. Zandona, M. Blazic, A.R. Jambrak, Whey Utilization: Sustainable Uses and Environmental Approach, Food Technol. Biotechnol. 59 (2021), 147-161. DOI: 10.17113/ftb.59.02.21.6968

(18) R. Mehra, H. Kumar, N. Kumar, S. Ranvir, A. Jana, H.S. Buttar, I.G. Telessy, C.G. Awuchi, C.O.R. Okpala, M. Korzeniowska, R.F.P. Guiné, Whey proteins processing and emergent derivatives: An insight perspective from constituents, bioactivities, functionalities to therapeutic applications, J. Funct. Foods. 87 (2021) 104760. DOI: 10.1016/J.JFF.2021.104760

(19) E. Arribas-López, N. Zand, O. Ojo, M.J. Snowden, T. Kochhar, The Effect of Amino Acids on Wound Healing: A Systematic Review and Meta-Analysis on Arginine and Glutamine, Nutrients 13 (2021), 2498. DOI: 10.3390/nu13082498.

(20) K. Khwaldia, C. Ferez, S. Banon, S. Desobry, J. Hardy, Milk proteins for edible films and coatings. Crit. Rev. Food Sci. Nutr. 44 (2004) 239–251. DOI: 10.1080/10408690490464906

(21) H. Chen, J. Wang, Y. Cheng, C. Wang, H. Liu, H. Bian, Y. Pan, J. Sun, W. Han, Application of Protein-Based Films and Coatings for Food Packaging: A Review, Polymers (Basel) 11 (2019) 2039. DOI: 10.3390/polym11122039.

(22) S. Kandasamy, J. Yoo, J. Yun, H.B. Kang, K.H. Seol, H.W. Kim, J.S. Ham, Application of Whey Protein-Based Edible Films and Coatings in Food Industries: An Updated Overview, Coatings. 11 (2021) 1056. DOI: 10.3390/coatings11091056

(23) H. Ebaid, A. Salem, A. Sayed, A. Metwalli, Whey protein enhances normal inflammatory responses during cutaneous wound healing in diabetic rats, Lipids Health Dis. 10 (2011) 235. DOI: 10.1186/1476-511X-10-235.

(24) O. Garraud, W. N. Hozzein, G. Badr, Wound healing: time to look for intelligent, 'natural' immunological approaches?, BMC Immunol. 18 (2017) 23. DOI: 10.1186/s12865-017-0207-y.

(25) P. Pino, S. Ronchetti, C. Mollea, M. Sangermano, B. Onida, F. Bosco, Whey Proteins–Zinc Oxide Bionanocomposite as Antibacterial Films. Pharmaceutics, 13 (2021) 1426. DOI: 10.3390/PHARMACEUTICS13091426

(26) H. Chopra, S. Bibi, S. Kumar, S.K. Muhammad, P. Kumar, I. Singh, Preparation and Evaluation of Chitosan/PVA Based Hydrogel Films Loaded with Honey for Wound Healing Application, Gels. 8 (2022) 111. DOI: 10.3390/gels8020111

(27) C. Ransy, C. Vaz, A. Lombès, F. Bouillaud, Use of H_2O_2 to Cause Oxidative Stress, the Catalase Issue, Int. J. Mol. Sci. 21 (2020) 9149. DOI: 10.3390/ijms21239149

(28) N. J. Anthis, G. M. Clore, Sequence-specific determination of protein and peptide concentrations by absorbance at 205 nm, Protein Sci. 22 (2013) 851-858. DOI: 10.1002/pro.2253. Epub 2013 Apr 29.

(29) A.P. Fraise, J. Maillard, S. Sattar, (Eds.), Russell, Hugo and Ayliffe's Principles and Practice of Disinfection, Preservation and Sterilization. 5th Edition, Wiley-Blackwell Publishing, 2012

(30) P. Grisoli, L. De Vita, C. Milanese, A. Taglietti, Y. Diaz Fernandez, M. Bouzin, L. D'Alfonso, L. Sironi, L., S. Rossi, B. Vigani, P. Sperandeo, A. Polissi, P. Pallavicini, PVA Films with Mixed Silver Nanoparticles and Gold Nanostars for Intrinsic and Photothermal Antibacterial Action, Nanomaterials (Basel). 11 (2021) 1387. DOI: 10.3390/nano11061387

(31) R. Podgórski, M. Wojasiński, T. Ciach, Nanofibrous materials affect the reaction of cytotoxicity assays, Sci. Rep. 12 (2022) 9047. DOI: 10.1038/s41598-022-13002-w

(32) M. Tenci, S. Rossi, M.C. Bonferoni, G. Sandri, C. Boselli, A. Di Lorenzo, M. Daglia, A. Icaro Cornaglia, L. Gioglio, C. Perotti, C. Caramella, F. Ferrari, Particulate systems based on pectin/chitosan association for the delivery of manuka honey components and platelet lysate in chronic skin ulcers, Int. J. Pharm. 509 (2016) 59-70. DOI:10.1016/j.ijpharm.2016.05.035

(33) L.C. Junqueira, W. Cossermelli, R. Brentani, Differential staining of collagens type I, II and III by Sirius Red and polarization microscopy, Arch. Histol. Jpn. 41 (1978) 267-74. DOI: 10.1679/aohc1950.41.267

(34) R. Lattouf, R. Younes, R., D. Lutomski, N. Naaman, G. Godeau, K. Senni, S. Changotade, Picrosirius red staining: a useful tool to appraise collagen networks in normal and pathological tissues, J. Histochem. Cytochem. 62 (2014) 751-758. DOI: 10.1369/0022155414545787

(35) O.B. Karaca, C.A. Oluk, T. Taşpinar, M. Güven, New Concept in Packaging: Milk Protein Edible Films. In: A. Malik, Z. Erginkaya, H. Erten (Eds), Health and Safety Aspects of Food Processing Technologies. Springer, Cham. 2019. DOI: 10.1007/978-3-030-24903-8_19

(36) J.M. Kassem, Future Challenges of Whey Proteins, Int. J. Dairy Sci. 10 (2015) 139–59. DOI:10.3923/IJDS.2015.139.159

(37) A.A. Hemmati, A. Larki-Harchegani, S. Shabib, A. Jalali, A. Rezaei, G. Housmand, Wound healing property of milk in full thickness wound model of rabbit, Int. J. Surg. 54 (2018) 133-140. DOI: 10.1016/j.ijsu.2018.04.030

(38) M.M. Agwa, S. Sabra, N.A. Atwa, H.A. Dahdooh, R.M. Lithy, H. Elmotasem, Potential of frankincense essential oil-loaded whey protein nanoparticles embedded in frankincense resin as a wound healing film based on green technology, J. Drug Deliv. Sci. Technol. 71 (2022) 103291. DOI: 10.1016/J.JDDST.2022.103291

(39) N. Melnikova, A. Knyazev, V. Nikolskiy, P. Peretyagin, K. Belyaeva, N. Nazarova, E. Liyaskina, D. Malygina, V. Revin, Wound Healing Composite Materials of Bacterial Cellulose and Zinc Oxide Nanoparticles with Immobilized Betulin Diphosphate, Nanomaterials (Basel). 11 (2021) 713. DOI: 10.3390/nano11030713

(40) D. Salarbashi, S. A. Mortazavi, M. S. Noghabi, B. S. F. Bazzaz, N. Sedaghat, M. Ramezani, I. Shahabi-Ghahfarrokhi, Development of new active packaging film made from a soluble soybean polysaccharide incorporating ZnO nanoparticles, Carbohydr. Polym. 140 (2016) 220-227. DOI: 10.1016/j.carbpol.2015.12.043

(41) P. Kanmani, J.-W. Rhim, Properties and characterization of bionanocomposite films prepared with various biopolymers and ZnO nanoparticles, Carbohydr. Polym. 106 (2014) 190-199. DOI: 10.1016/j.carbpol.2014.02.007.

(42) J. A. A. Abdullah, M. Jimenez-Rosado, A. Guerrero, A. Romero, Biopolymer-Based Films Reinforced with Green Synthesized Zinc Oxide Nanoparticles, Polymers (Basel) 14 (2022) 5202. DOI: 10.3390/polym14235202.

(43) P. Kanmani, J.W. Rhim, Properties and characterization of bionanocomposite films prepared with various biopolymers and ZnO nanoparticles, Carbohydr. Polym. 106 (2014) 190-199. DOI: 10.1016/j.carbpol.2014.02.007

(44) M.T. Khorasani, A. Joorabloo, A. Moghaddam, H. Shamsi, Z. Mansoori Moghadam, Incorporation of ZnO nanoparticles into heparinised polyvinyl alcohol/chitosan hydrogels for wound dressing application, Int. J. Biol. Macromol. 114 (2018) 1203-1215. DOI: 10.1016/j.ijbiomac.2018.04.010

(45) S. Roy, J.W. Rhim, Carrageenan-Based Antimicrobial Bionanocomposite Films Incorporated with ZnO Nanoparticles Stabilized by Melanin, Food Hydrocoll. 90 (2019) 500–507. DOI:10.1016/J.FOODHYD.2018.12.056

(46) Q. Du, P. Zhou, Y. Pan, X. Qu, L. Liu, H. Yu, J. Hou, Influence of hydrophobicity and roughness on the wetting and flow resistance of water droplets on solid surface: A many-body dissipative particle dynamics study, Chem. Eng. Sci. 249 (2022) 117327. DOI: 10.1016/j.ces.2021.117327

(47) X. Liu, T. Lin, J. Fang, G. Yao, H. Zhao, M. Dodson, X. Wang, In vivo wound healing and antibacterial performances of electrospun nanofibre membranes, J. Biomed. Mater. Res. A. 94 (2010) 499-508. DOI:10.1002/jbm.a.32718

(48) K. Kalantari, M. Ebrahim, B. Saleh, P. Soltantabar, T.J. Webster, Chitosan/PVA Hydrogels Incorporated with Green Synthesized Cerium Oxide Nanoparticles for Wound Healing Applications, Eur. Polym. J. 134 (2020) 109853. DOI:10.1016/J.EURPOLYMJ.2020.109853

(49) D. George, P.U. Maheswari, K.M.M.S. Begum, Chitosan-cellulose hydrogel conjugated with L-histidine and zinc oxide nanoparticles for sustained drug delivery: Kinetics and in-vitro biological studies, Carbohydr. Polym. 236 (2020) 116101. DOI: 10.1016/j.carbpol.2020.116101

(50) M.E. Villanueva, M.L. Cuestas, C.J. Pérez, V. Campo Dall'Orto, G.J. Copello, Smart release of antimicrobial ZnO nanoplates from a pH-responsive keratin hydrogel, J. Colloid. Interface Sci. 536 (2019) 372-380. DOI: 10.1016/j.jcis.2018.10.067

(51) M. Mori, S. Rossi, F. Ferrari, M.C. Bonferoni, G. Sandri, T. Chlapanidas, M.L. Torre, C. Caramella, Sponge-Like Dressings Based on the Association of Chitosan and Sericin for the Treatment of Chronic Skin Ulcers. I. Design of Experiments-Assisted Development, J. Pharm. Sci. 105 (2016) 1180-1187. DOI: 10.1016/j.xphs.2015.11.047

(52) M.M. Gonçalves, J. Carneiro, B. Justus, J.T. Espinoza, J. M. Budel, P.V. Farago, J.P.D. Paula, Preparation and Characterization of a Novel Antimicrobial Film Dressing for Wound Healing Application, Braz. J. Pharm. Sci. 56 (2021). DOI:10.1590/S2175-97902020000118784

683 (53) P.I. Morgado, A. Aguiar-Ricardo, I.J. Correia, Asymmetric Membranes as Ideal Wound
684 Dressings: An Overview on Production Methods, Structure, Properties and Performance
685 Relationship, J. Membr. Sci. 490 (2015) 139–151. DOI:10.1016/J.MEMSCI.2015.04.064

686 (54) W.C. Lin, C.C. Lien, H.J. Yeh, C.M. Yu, S.H. Hsu, Bacterial cellulose and bacterial
687 cellulose-chitosan membranes for wound dressing applications, Carbohydr. Polym. 94
688 (2013) 603-611. DOI: 10.1016/j.carbpol.2013.01.076

689 (55) B. Vigani, C. Valentino, V. Cavalloro, L. Catenacci, M. Sorrenti, G. Sandri, M.C.
690 Bonferoni, C. Bozzi, S. Collina, S. Rossi, F. Ferrari, Gellan-Based Composite System as a
691 Potential Tool for the Treatment of Nervous Tissue Injuries: Cross-Linked Electrospun
692 Nanofibers Embedded in a RC-33-Loaded Freeze-Dried Matrix, Pharmaceutics. 13 (2021)
693 164. DOI: 10.3390/pharmaceutics13020164

694 (56) S. Keshavarzi, A. Babaei, A. Goudarzi, A. Shakeri, ZnO nanoparticles as chain elasticity
695 reducer and structural elasticity enhancer: Correlating the degradating role and localization
696 of ZnO with the morphological and mechanical properties of PLA/PP/ZnO nanocomposite,
697 Polym. Adv. Technol. 30 (2019) 1083–1095. DOI: 10.1002/pat.4542

698 (57) M. Schäfer, S. Werner, Oxidative stress in normal and impaired wound repair,
699 Pharmacol. Res. 58 (2008) 165-171. DOI: 10.1016/j.phrs.2008.06.004

700 (58) B. Vigani, S. Rossi, G. Sandri, M.C. Bonferoni, M. Rui, S. Collina, F. Fagiani, C. Lanni,
701 F. Ferrari, Dual-Functioning Scaffolds for the Treatment of Spinal Cord Injury: Alginate
702 Nanofibers Loaded with the Sigma 1 Receptor (S1R) Agonist RC-33 in Chitosan Films,
703 Mar. Drugs. 18 (2019) 21. DOI: 10.3390/md18010021

(59) K. Khwaldia, S. Banon, S. Desobry, J. Hardy, Mechanical and barrier properties of sodium caseinate–anhydrous milk fat edible films, JFST. 39 (2004) 403-411. DOI: 10.1111/j.1365-2621.2004.00797.x

(60) A.K. Ghosh, B. Prasun, Polysaccharide-Protein Interactions and Their Relevance in Food Colloids. In: D.N. Karunaratne, (Ed), The Complex World of Polysaccharides. IntechOpen, 2012. DOI: 10.5772/50561

(61) E. Yuan, M. Zhou, S. Nie, J. Ren, Interaction mechanism between ZnO nanoparticles-whey protein and its effect on toxicity in GES-1 cells, J. Food Sci. 87 (2022) 2417-2426. DOI: 10.1111/1750-3841.16193.

(62) W. Zhang, M. A. Sani, Z. Zhang, D. J. Clements, S. M. Jafari, High performance biopolymeric packaging films containing zinc oxide nanoparticles for fresh food preservation: A review, Int. J. Biol. Macromol. 230 (2023) 123188. DOI: 10.1016/j.ijbiomac.2023.123188.

(63) P.J.P. Espitia, N.F.F. Soares, J.S.R. Coimbra, N.J. de Andrade, R.S. Cruz, E.A.A. Mederiros, Zinc Oxide Nanoparticles: Synthesis, Antimicrobial Activity and Food Packaging Applications, Food Bioprocess. Technol. 5 (2012) 1447–1464. DOI: 10.1007/s11947-012-0797-6

(64) M. Gupta, V.K. Mahajan, K.S. Mehta, P.S. Chauhan, Zinc therapy in dermatology: a review, Dermatol. Res. Pract. (2014) 709152. DOI: 10.1155/2014/709152

(65) I. Wessels, M. Maywald, L. Rink, Zinc as a Gatekeeper of Immune Function. Nutrients. 9 (2017) 1286. DOI: 10.3390/nu9121286

(66) A.J. Singer, R.A.F. Clark, Cutaneous Wound Healing. Edited by Franklin H. Epstein 341 (1999), 738–46. DOI:10.1056/NEJM199909023411006.